**Supporting Information**

# Amorphous Mesoporous Magnesium Carbonate (MMC) as a functional support for UV blocking semiconductor nanoparticles for cosmetic applications

Michelle Åhlén, Ocean Cheung* and Maria Strømme*

Division of Nanotechnology and Functional Materials, Department of Engineering Sciences, Uppsala University, SE-751 21, Uppsala, Sweden

## EXPERIMENTAL

## MATERIALS

Talcum USP grade median particle size 5.5 µm Making Cosmetics, Potato starch food grade Garant, Magnesium hydroxide BioUltra ≥99.0% (KT) Sigma-Aldrich.

All chemicals were used as bought without further purification.

## RESULTS AND DISCUSSION

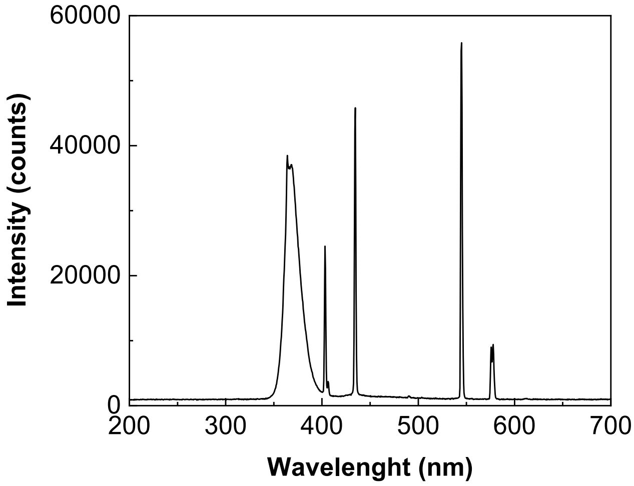


**Figure S1.** Emission spectrum of four UV-9W-L G23 type fluorescence tubes used for photocatalysis experiment.

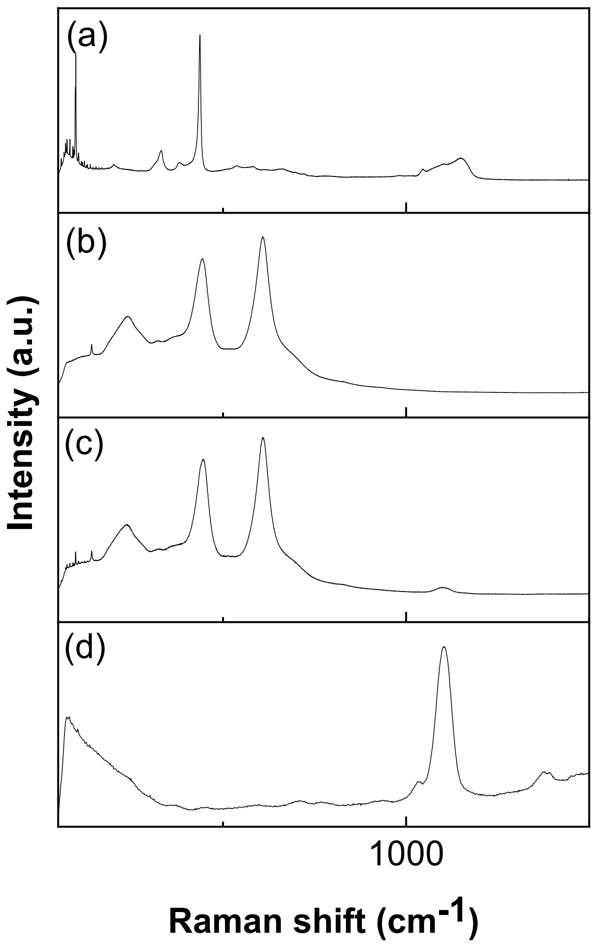


**Figure S2.** Raman spectra of (a) ZnO (wurtzite) nanoparticles, (b) $TiO_2$ (rutile) nanoparticles, (c) MMC-$TiO_2$-ZnO and (d) MMC.

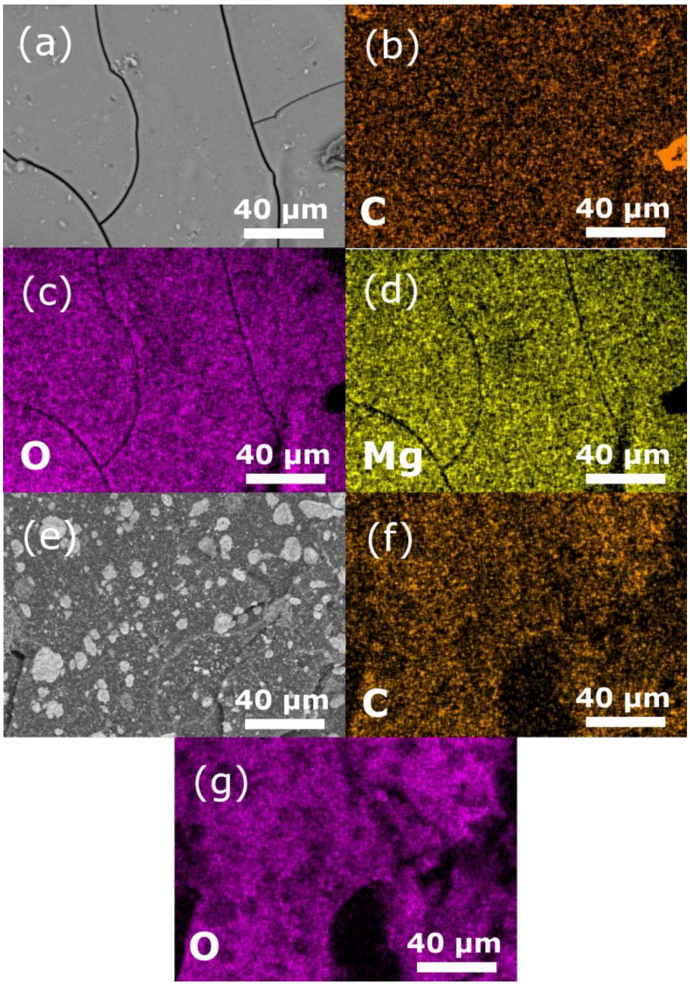


**Figure S3.** SEM-EDX maps of (a-d) MMC and (e-g) MMC-$TiO_2$-ZnO on the elements carbon, oxygen and magnesium.

**Table S1.** Estimated elemental analysis of MMC and MMC-TiO2-ZnO obtained from SEM-EDX mappings of the areas shown in Figure S4.

| Element | MMC (at. %) | MMC-$TiO_2$-ZnO (at. %) |
|---|---|---|
| Oxygen | 64.6 ± 8.0 | 60.9 ±5.6 |
| Carbon | 18.7 ± 2.0 | 17.5 ± 1.4 |
| Magnesium | 16.8 ± 1.6 | 13.5 ± 1.0 |
| Titanium | — | 4.1 ± 0.3 |
| Zinc | — | 4.0 ± 0.5 |

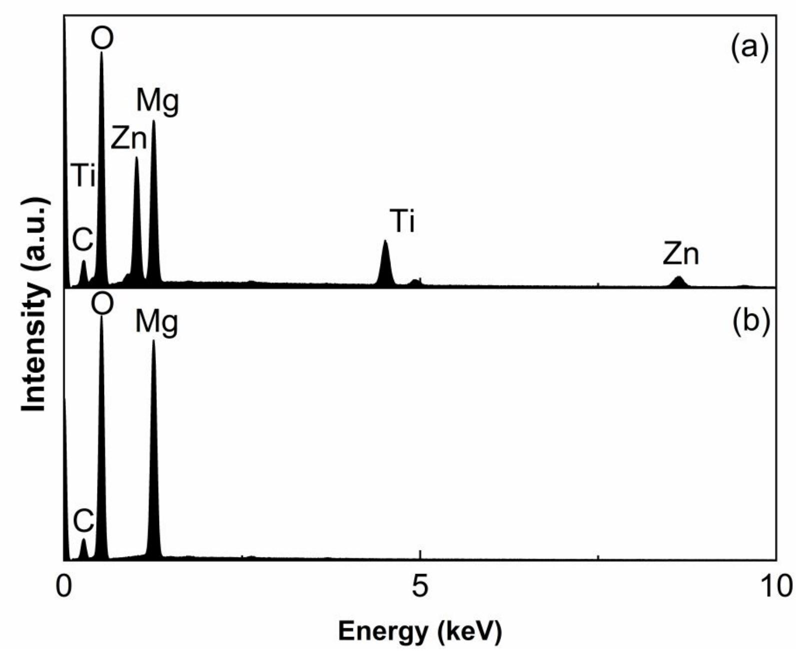


**Figure S4**. SEM-EDX spectra of (a) MMC-TiO2-ZnO and (b) MMC.

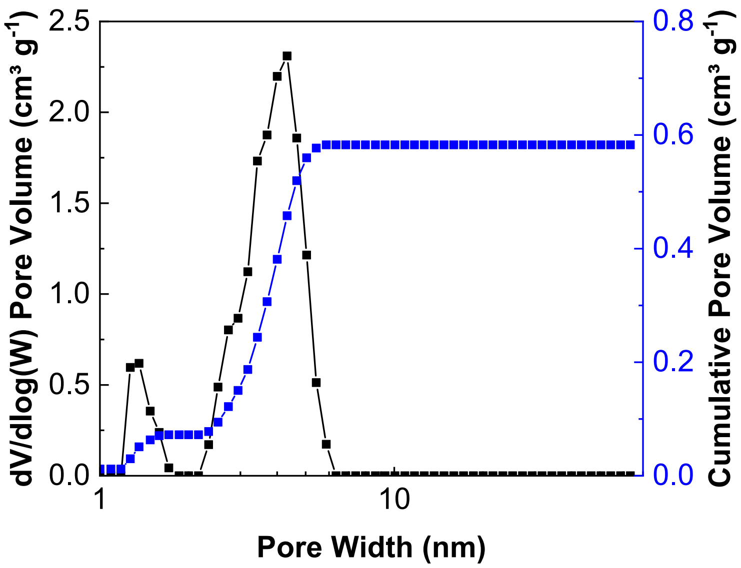


**Figure S5.** Differential pore volume distribution (■) and cumulative pore volume (●) of MMC.

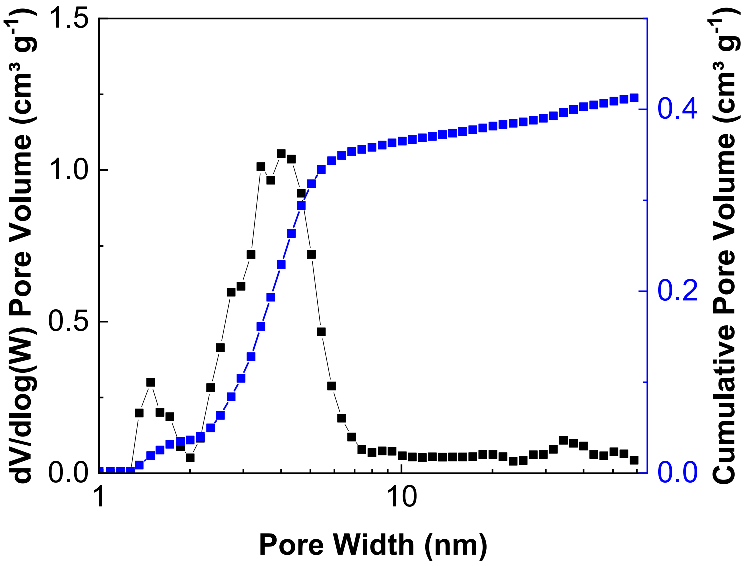


**Figure S6.** Differential pore volume distribution (■) and cumulative pore volume (●) of MMC-$TiO_2$-ZnO.

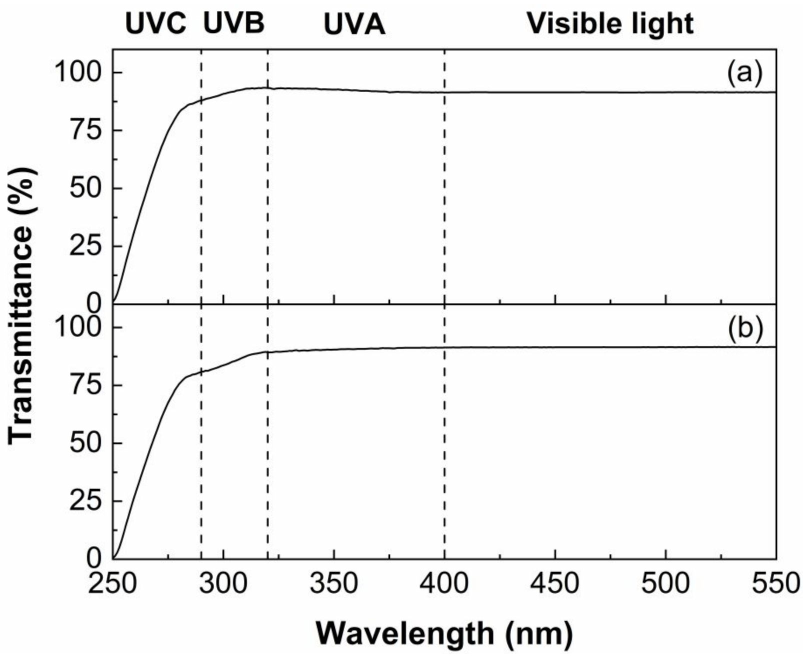


**Figure S7.** UV-transmittance of (a) a PDMS covered PMMA plate and (b) a PMMA plate.

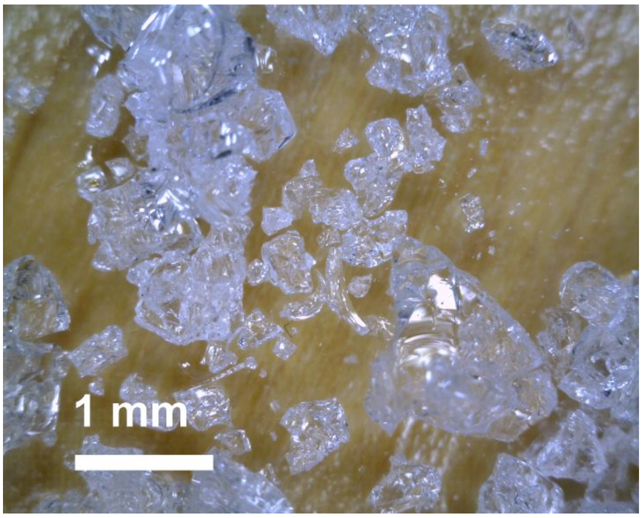


**Figure S8.** Light microscopy image of MMC particles.

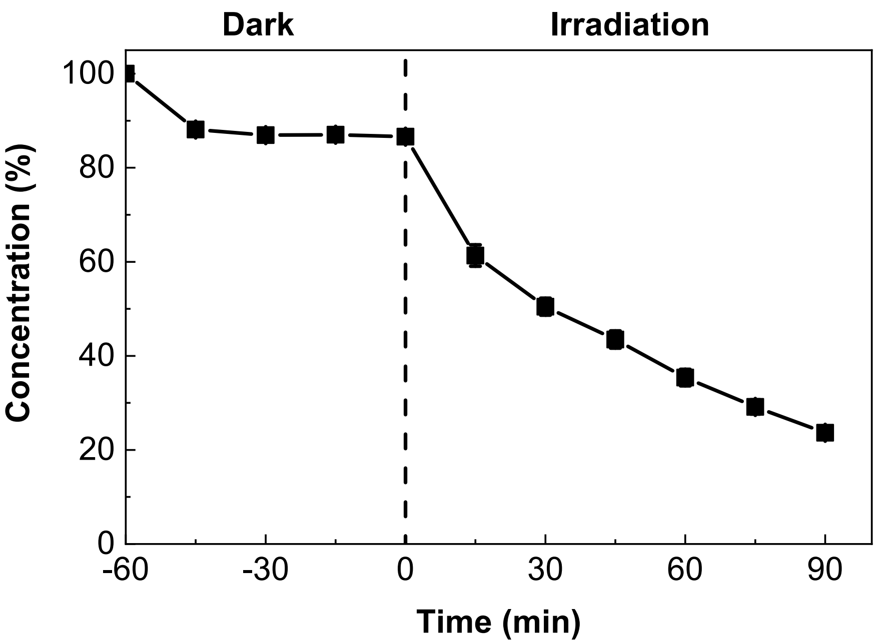


**Figure S9.** The effect of talc mixed with $TiO_2$ (rutile) and ZnO nanoparticles on the adsorption and photocatalytic degradation of the anionic azo dye amaranth. The mixture contained an equal amount of $TiO_2$/ZnO as MMC-$TiO_2$-ZnO and the measurements were performed in triplicates.

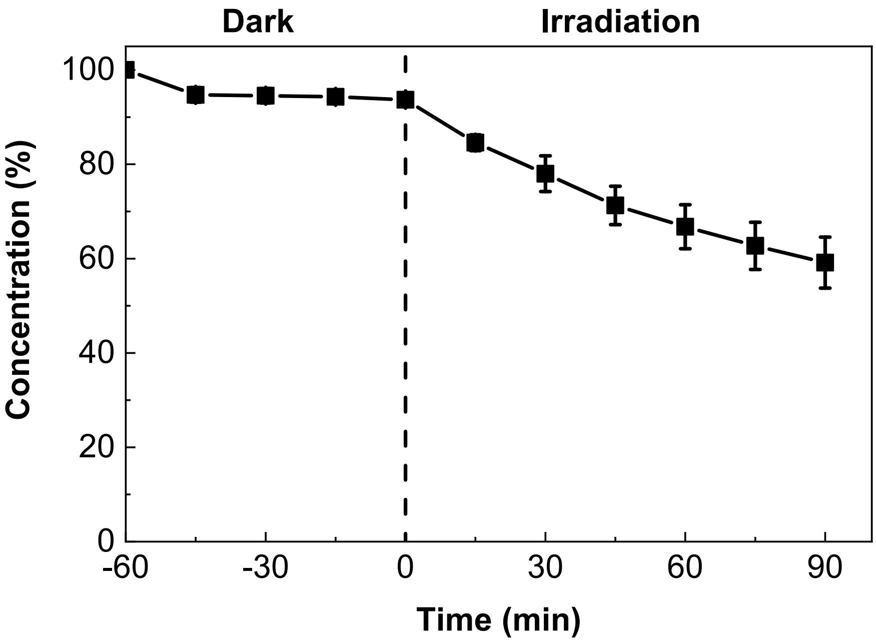


**Figure S10.** The effect of starch mixed with $TiO_2$ (rutile) and ZnO nanoparticles on the adsorption and photocatalytic degradation of the anionic azo dye amaranth. The mixture contained an equal amount of $TiO_2$/ZnO as MMC-$TiO_2$-ZnO and the measurements were performed in triplicates.

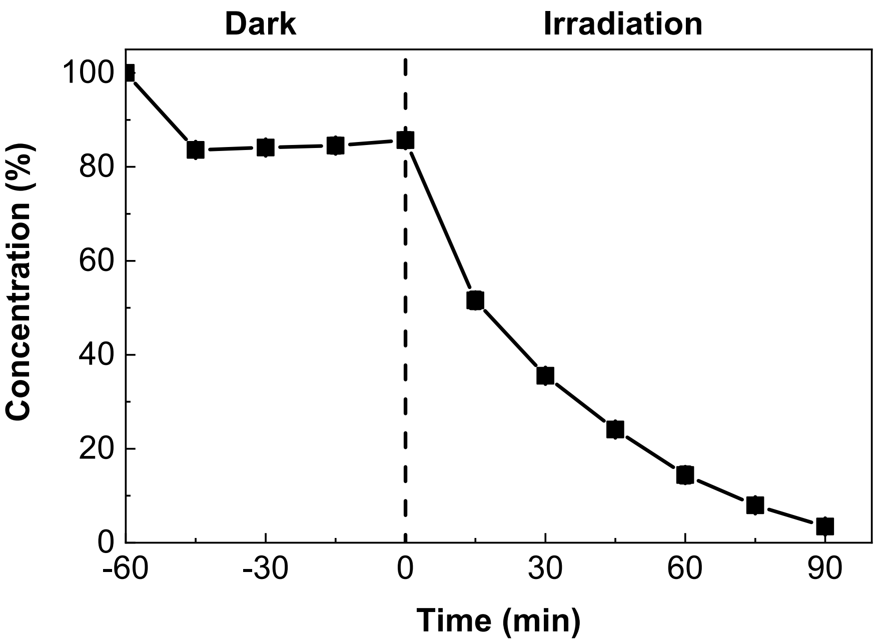


**Figure S11.** The effect of $Mg(OH)_2$ mixed with $TiO_2$ and ZnO nanoparticles on the adsorption and photocatalytic degradation of the anionic azo dye amaranth. The mixture contained an equal amount of $TiO_2$/ZnO as MMC-$TiO_2$-ZnO and the measurements were performed in triplicates.

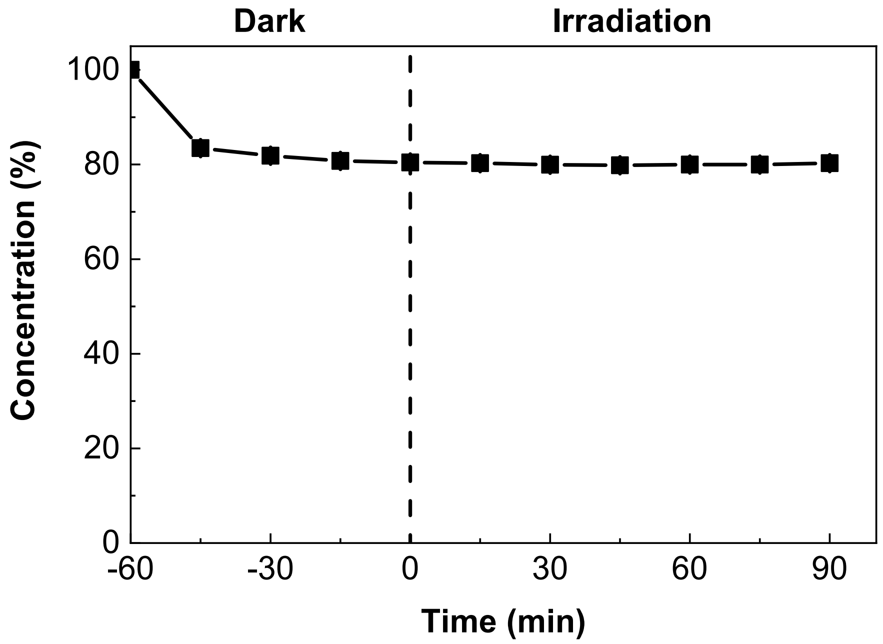


**Figure S12.** The effect of $MgCO_3$ on the adsorption and photocatalytic degradation of the anionic azo dye amaranth. The measurements were performed in triplicates.

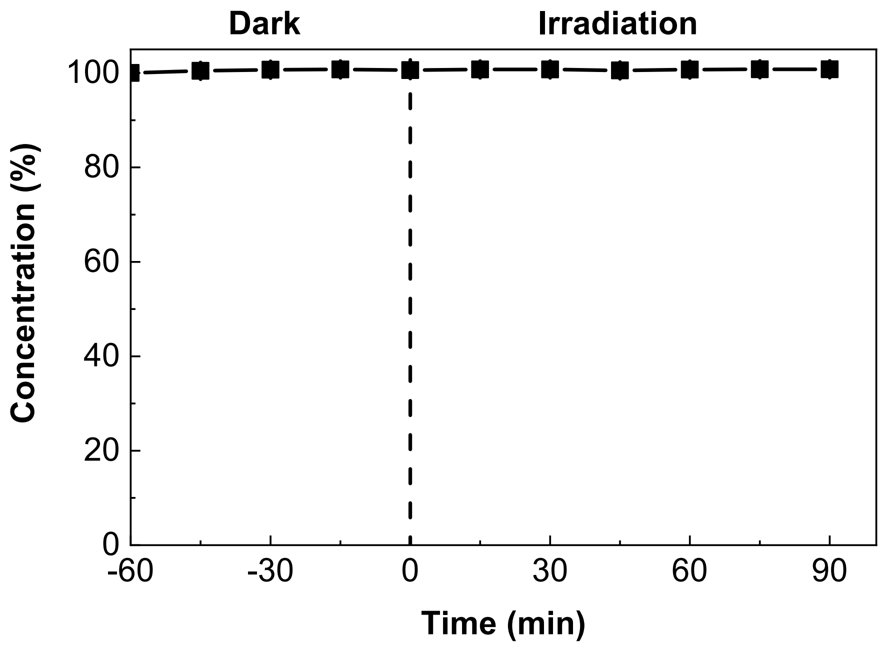


**Figure S13.** The effect of starch on the adsorption and photocatalytic degradation of the anionic azo dye amaranth. The measurements were performed in triplicates.

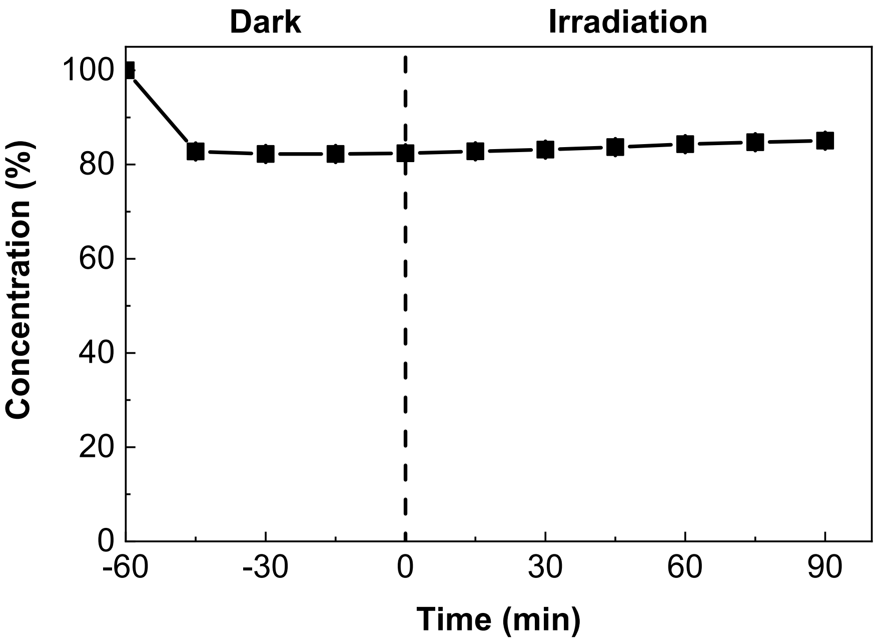


**Figure S14.** The effect of $Mg(OH)_2$ on the adsorption and photocatalytic degradation of the anionic azo dye amaranth. The measurements were performed in triplicates.

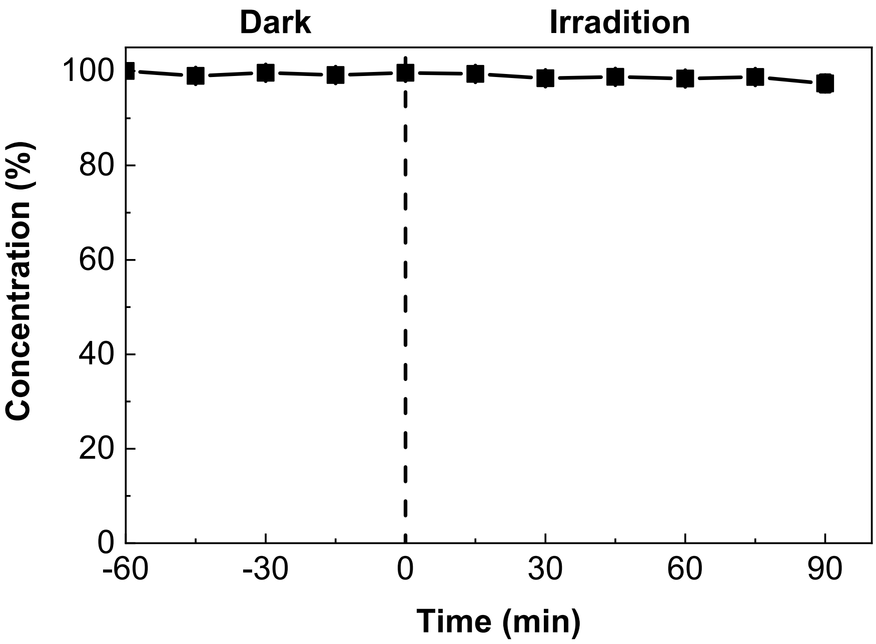


**Figure S15.** The effect of talc on the adsorption and photocatalytic degradation of the anionic azo dye amaranth. The measurements were performed in triplicates.